A comparative study dedicated to rotor failure detection in induction motors using MCSA, DWT, and EMD techniques

Salim Sbaa, Noureddine Bessous, Remus Pusca, Raphael Romary

▶ **To cite this version:**

Salim Sbaa, Noureddine Bessous, Remus Pusca, Raphael Romary. A comparative study dedicated to rotor failure detection in induction motors using MCSA, DWT, and EMD techniques. 2020 International Conference on Electrical Engineering (ICEE), Sep 2020, Istanbul, Turkey. pp.1-11, 10.1109/ICEE49691.2020.9249774 . hal-04296850

HAL Id: hal-04296850

https://univ-artois.hal.science/hal-04296850

Submitted on 10 Jan 2024

HAL is a multi-disciplinary open access archive for the deposit and dissemination of scientific research documents, whether they are published or not. The documents may come from teaching and research institutions in France or abroad, or from public or private research centers.

L'archive ouverte pluridisciplinaire **HAL**, est destinée au dépôt et à la diffusion de documents scientifiques de niveau recherche, publiés ou non, émanant des établissements d'enseignement et de recherche français ou étrangers, des laboratoires publics ou privés.

A comparative study dedicated to rotor failure detection in induction motors using MCSA, DWT, and EMD techniques

Salim Sbaa[1], Noureddine Bessous[2]
[1,2]Department of electrical engineering
[1]University of Mohammed Khider, Biskra
Biskra 07000, Algeria
[2]University of El-Oued, Algeria
El-Oued 39000, Algeria
nbessous@yahoo.fr, s_sbaa@yahoo.fr

Remus Pusca, Raphael Romary
Laboratory of Electrotechnical and Environmental Systems (LSEE)
University of Artois, France
Béthune, France, Univ. Artois, EA 4025 LSEE, F-62400, Béthune, France
remus.pusca@univ-artois.fr, raphael.romary@univ-artois.fr

Abstract— **This paper presents the detailed detection of broken rotor bar faults in squirrel cage induction motors (SCIMs). This study used three diagnostic techniques. Early faults detection allows us to avoid catastrophic damage. In this work, we have exploited the stator current signal by three recent methods. The first technique uses the fast Fourier transform (FFT) which is often called motor current signature analysis (MCSA or MCSA-FFT). According to this technique, we carefully checked the spectral content of the stator current. In addition, we have clearly noticed to new harmonics that indicate the broken rotor bar (BRB) faults exists. The second technique is based on the discrete wavelet transform (DWT); this technique is widely used in the diagnosis field of rotating machinery. In order to detect the BRB faults in SCIMs, we have exploited this method by three important indicators. One of them is based on the mean square error (MSE) of each detail coefficient. In this study, we applied a new indicator (MSE) for the BRB fault detection based on DWT. The last method is empirical mode decomposition (EMD) to perform the current signature analysis in order to decompose the motor current signal into intrinsic mode functions (IMFs). It is currently competing with several methods such as: MCSA, DWT, etc. So, it is possible to detect BRBs through the evaluation of the different IMF levels for both conditions, healthy and faulty state of SCIM. An experimental test for different conditions: at no load or at load operation, healthy or faulty state of the induction motor has been performed. So, experimental results using three methods showed a detailed comparison between them in order to achieve a judicious decision on the broken rotor bars detection. Finally, we have confirmed the proposals ideas in this subject in order to detect the broken rotor bar faults.**

Keywords- Broken rotor bar faults; Discrete wavelet transform; Empirical mode decomposition; Motor current signature analysis; Discrete wavelet transform

I. INTRODUCTION

Squirrel cage induction motors (SCIMs) are widely used in the industry. They are self-starting, simple, robust and maintain a reasonably constant speed from low load to full load, set by the frequency of the power supply and the number of poles of the stator winding. This simplifies the application and replacement of these motors. Almost 95% of the induction motors used is of squirrel cage type. Faults in SCIMs can be classified by: stator faults and rotor faults. Among them, we mention:

- Stator faults such as: opening of a phase, short circuit of the coils, eccentricity of the stator, etc. [1-2].
- Rotor faults such as: rotor eccentricity, bearing problem, breakage of bars, etc. [3-4].

These faults produce some symptoms such as air-gap variation, increased losses in efficiency, unbalanced voltages and/or line currents, decreased average torque, increased torque pulsations, excessive heating, etc. Generally, the anomaly of electromagnetic field in the air-gap creates sidebands harmonic components in the stator current spectra [5,7]. The verification of some sideband frequencies can be used as a good indicator to BRB faults detection.

Researchers have used several success techniques as the fast Fourier transform in vibration signal, current signal, electromagnetic torque signal, speed signal, etc. in order to detect different faults in the rotating electrical machinery [8,12].

Several methods have been used to detect the BRB faults in SCIMs such as: motor vibration signature analysis (MVSA), wavelet transforms, fuzzy logic technique, artificial neural network (ANN), and motor current signature analysis by FFT (MCSA-FFT), etc. [13,17].

MCSA-FFT is recently widely used in the field of the faults detection in SCIMs [18-19]. This method and as it benefits, it also has many disadvantages. As the FFT has many limitations in no-stationary regime, this study will carefully explain this problem with logical arguments.

This work will be applied the MCSA in order to detect the BRB faults. We will try to do a very detailed check about the characteristic frequencies for the BRB faults.

This study is based on the realization of a motor setup which allows us to measure the stator current and to analyse it carefully.

Advanced signal processing methods as Continuous and/or Discrete Wavelet Transform (CWT, DWT), Wavelet Packet Transform (WPT), Hilbert Transform (HT), Empirical Mode Decomposition (EMD), etc. have been used to detect many faults in SCIMs [20-21]. The door is open according to the development of signal processing software to fault diagnosis in rotating electrical machinery.

The discrete wavelet transform technique (DWT) is applied with detailed way. We have defined here a new estimator called mean square error (MSE).

In the presence of nonlinear and non-stationary data, the EMD has the attractive feature of robustness. It is obvious that appropriate treatment by the EMD system can yield adequate results [22,24].

Our work will analyze the BRB faults based on the EMD technique, and exactly on the comparison between the intrinsic mode functions (IMFs).

The experimental results presented here help us to measure the stator current signal under different conditions (healthy motor, faulty motor, at-load operation, at 75% of the load operation).

So in this study, we will try to compare the effectiveness of three interesting techniques in diagnosis field.

II. Motor Test Bench

In this study, we have used a squirrel cage induction motor (SCIM) which has a characteristic as follow: 3kW, 2-pole, f_s=50Hz, 28 bars. Fig.1 shows the SCIM with some equipment dedicated to the data acquisition.

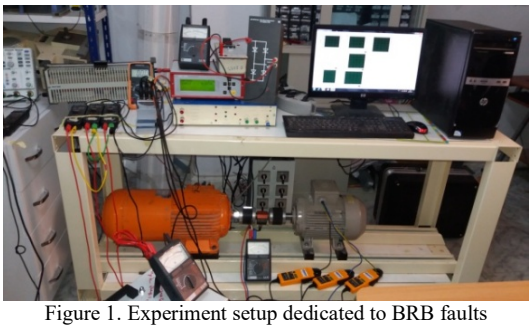

Figure 1. Experiment setup dedicated to BRB faults

We realized a 1 BRB and 2 BRBs in order to study the severity phenomenon. Fig. 2 shows the photos of healthy and faulty rotor of SCIM.

Figure 2. Photos of healthy and faulty rotor bars

III. Detection of broken Rotor Bars Using MCSA-FFT

Diagnosis of SCIM by stator current spectral content lead to detect the BRB defects by the sideband components. The additional harmonics are provided as follow [5]:

$$f_{BRBs} = (1 \pm 2ks).f_s \quad (1)$$

where, k=1,2,3, ..., s is the slip of the induction motors.

On the other hand, frequencies can appear in the stator current spectrum can be writing as follows [25-26]:

$$f_{BRBs} = \left[(6k \pm 1) \pm 2ks\right] f_s \quad (2)$$

where, k=1,2,3, ..., s is the slip of the induction motors.

We can notice that the frequencies of orders: 5, 7, 11, 17, 19, 23, 25, … (6k±1) have the frequencies: (6k±1)×f_s.

As these harmonics are introduced in magneto-motive force (FMM), they affected under the existence of the BRB faults and/or the slip value. The formula above shows the values of other frequencies called sideband frequencies (SBFs).

The harmonics of the stator current of frequency (6k±1)×f_s are modulated in amplitude at the frequency 2×(6k±1)×sf_s.

Another series of harmonics can be found in the stator current spectrum as a result of BRB defects, they are given as follows:

$$f_{BRBs} = \left[\frac{k}{p}(1-s) \pm s\right].f_s \quad (3)$$

with, (k/p=1, 5, 7, 11,…)

Mixed eccentricity of rotor is always present even for a new SCIM. The characteristic frequencies of mixed eccentricity are given by:

$$f_{mix-ecc} = \left|f_s \pm kf_r\right| \quad (4)$$

where, k=1,2,3, ...

A. 0% of the load operation of SCIM

Fig. 3 shows the stator current spectrum in case of operating at 0% of the load (s≈0). We do not find any additional frequency in the stator current spectrum. However, our SCIM is under rotor one broken bar. We explain the absence of the characteristic frequencies by the slip value which is close to zero. So, it is difficult to detect the BRB faults in induction motor at no load by the MCSA-FFT.

In most cases we see the frequencies because of the mixed eccentricity of the rotor. Among them, and for s≈0 we indicate to: $f_{mix\text{-}ecc(-)}$ =25.1 Hz and $f_{mix\text{-}ecc(+)}$= 74.9 Hz in the case where k=1.

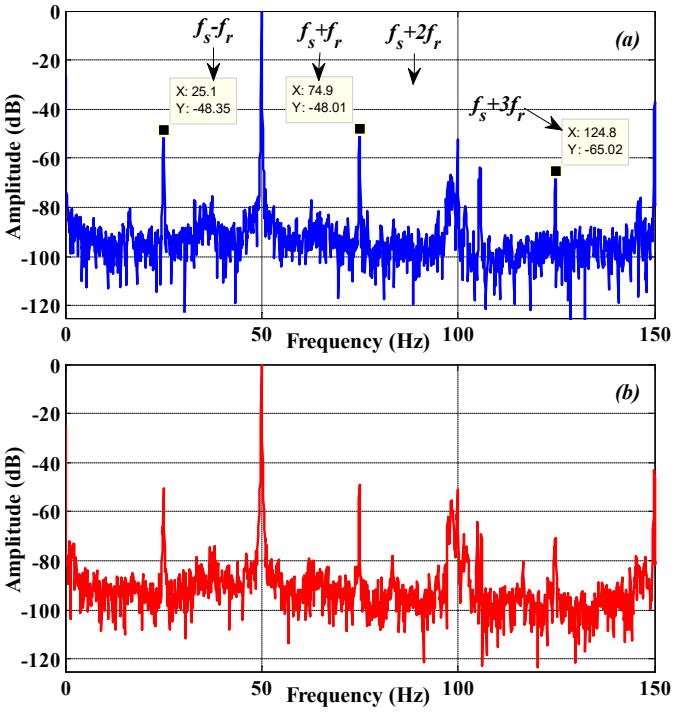

Figure 3. Stator current spectrum at 0% load (0-150Hz)

Fig. 4 shows the same remarks around frequency 5 and 7; and no frequency appears in this area.

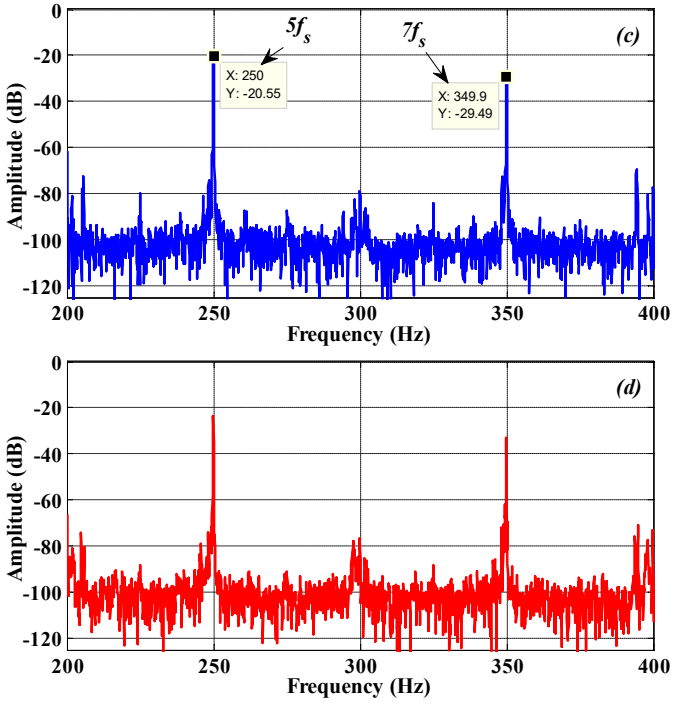

Figure 4. Stator current spectrum at 0% load (200-400Hz)

We notice that the stator current spectrum does not have a change in harmonic content at no load motor. In this case, the additional frequencies caused by BRB faults are almost invisible; this is due to the s≈0.

For the slip value equal zero (s = 0); we found $2\times s\times f_s = 0$. In this case the characteristic frequencies of the BRB faults will be invisible.

B. 75% of the load operation of SCIM

We know that the variation of the load affects in the slip value. In this part, we apply a resistant torque which ensures a load of 75% (s = 3.6%).

We can verify that the BRB faults induce SBFs around the fundamental (f_s) and the harmonics 5, 7 and the *RSHs*.

Fig. 5 shows the SBFs in which the frequencies move with the slip value. Components of values $(1\pm 2ks)\times f_s$ and others, are characterize this type of fault.

The additional harmonics around the supply frequency, 5, 7, and *RSHs* characterize the BRB faults (Table I).

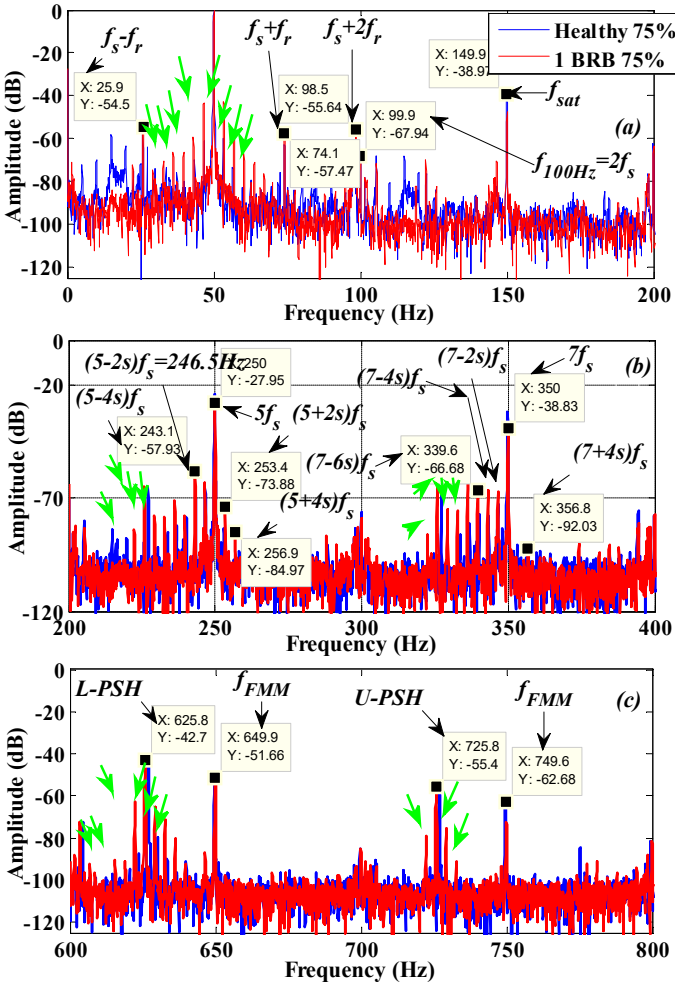

Figure 5. Stator current spectrum at 75% of load; (a): 0-200 Hz, (b): 200-400 Hz, (c): 600-800 Hz

The sidebands presented in Fig. (6-a) verify the formula (7). Other sidebands around the rotor slot harmonics (*RSHs*) were verified in Fig. (6-c). These frequencies are attached with RSHs and spaced by $2\times s\times f_s$; we therefore conclude to the following formula:

$$f_{BRB-RSHs} = RSH \pm 2ksf_s \quad (5)$$

We can see the frequency components at f_s-f_r, f_s+f_r, f_s+2f_r, etc. which are already exist in the spectrum of the healthy machine due to mixed eccentricity.

In addition, frequencies due to saturation (f_{sat}) appeared on the spectrum of experimental results. These frequencies have important amplitudes.

$$f_{sat} = 3kf_s \quad (6)$$

where, k is an odd number.

It's remarkable in two states conditions (healthy and faulty motor), the appearance of the double component of the supply frequency f_{doub}=100 Hz, it has the value:

$$f_{doub-s} = f_{100Hz} = 2f_s \quad (7)$$

Some other frequency bands are shown in these figures :

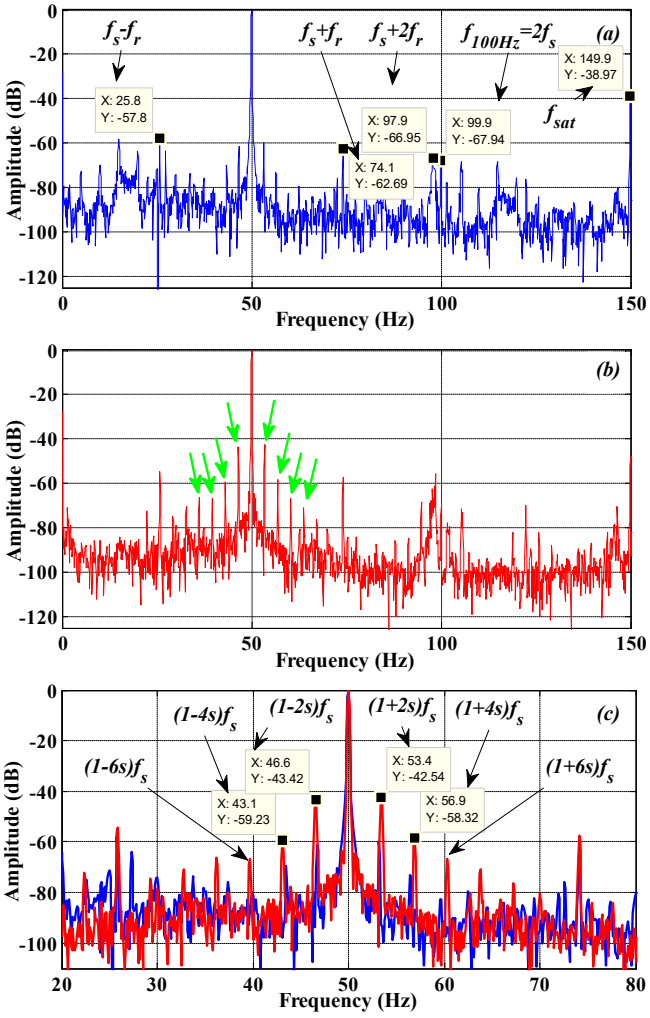

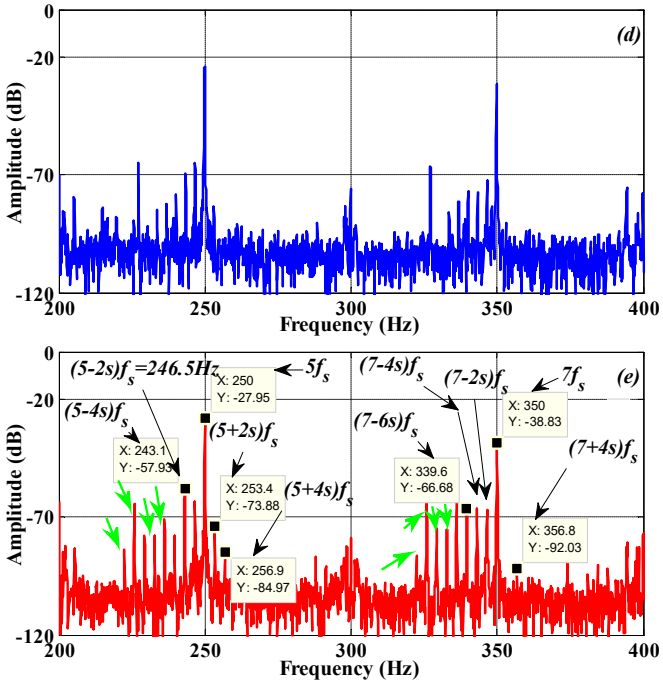

Figure 6. Stator current spectrum at 75% of load; (a), (b), (c): Around f_s and (d), (e): Around 5, 7

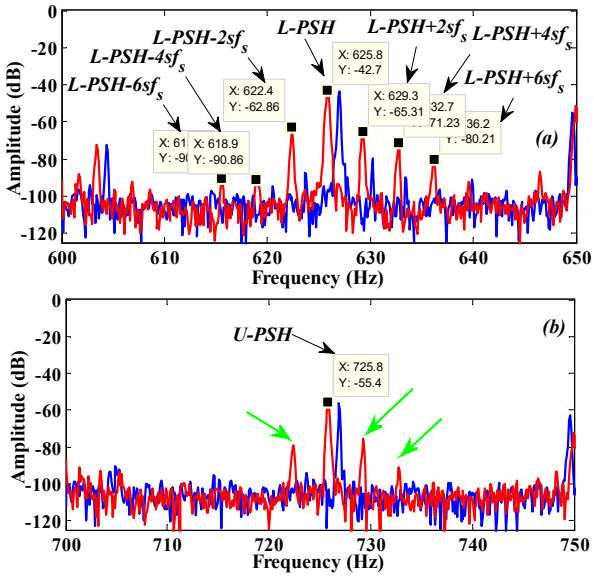

Figure 7. Stator current spectrum at 75% of load; (a): Around *L-PSH* and (b): Around *U-PSH*

TABLE I. Harmonics of the stator current spectrum (1BRB)

Formulas of characteristic frequencies	Theoretical values (Hz)	Experimental values (Hz)	Amplitude «healthy» (dB)	Amplitude « 1BRB » (dB)
(1-2s)f_s	46.4 Hz	46.6 Hz	-61.7	**-43.42**
(1+2s)f_s	53.6 Hz	53.4 Hz	-59.67	**-42.54**
5f_s	250 Hz	250 Hz	-23.91	**-27.95**
(5-2s)f_s	246.4 Hz	246.5 Hz	-65.15	**-63.36**
(5+2s)f_s	253.6 Hz	253.4 Hz	-83.2	**-73.88**
7f_s	350 Hz	350 Hz	-31.51	**-38.83**

$RSH_1^{(-)} - 2sf_s$	621.2 Hz	622.4 Hz	-87.38	**-62.86**
$RSH_1^{(-)} + 2sf_s$	628.4 Hz	629.3 Hz	-79.64	**-65.31**

We see in this study the following two remarks:

- The absence of the characteristic frequencies under BRB faults at no-load operation.
- Returning to figures (5) and (6), we clearly notice the existence of sidebands of harmonics in the healthy state of the machine.

IV. DETECTION OF BRB FAULTS USING DWT

The development of monitoring systems for rotating machines is not only for detecting failures, but also for how these failures can be quickly detected.

The purpose of this part is to present an experimental study of the BRB faults in the induction motor and under different load conditions which is based on an analysis of the discrete wavelet transform.

Raising the original signal from the stator current, or any signal, requires a preprocessing platform.

The discrete wavelet transform (DWT) can make a very adequate and effectiveness of signals analysis.

DWT based on a successive operation from a high-pass filter (HP), and low pass filter (LP) which leads to find the approximation (a_i) and details (d_i). Each step is conducted to the first level. One of two results is the approximation *a1* and the other is the detail *d1*. *a1* is the approximate shape of the original signal without noise, and *d1* is the detailed shape of the signal that influences on original signal (noise).

Fig. 8 shows the discrete wavelet transform scheme.

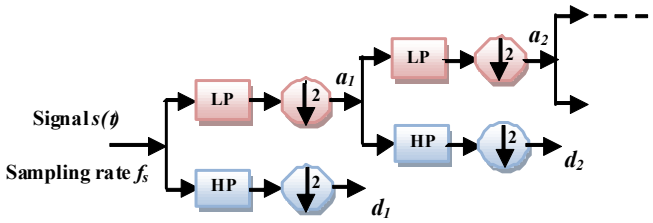

Figure 8. Discrete wavelet decomposition scheme

Our study is based on the MCSA by DWT under a sampling frequency equal to 12800Hz. The fault detection is based on a precise analysis and a detailed comparison between the decomposition levels (di or ai).

These decompositions are limited by the number N_{LL}:

$$N_{LL} = \text{int}\left[\frac{\log\left(\frac{f_{sa}}{f_s}\right)}{\log(2)}\right] \quad (8)$$

f_{sa}=12.8Hz, f_s=50Hz are the sampling frequency used for experimental recovery and fundamental frequency respectively.

[27] and [28] have detailed the choice of the mother wavelet and the adequate number for decomposition levels.

In addition, [28] has well presented the reason of the threshold of the levels and the limit of order for various signals like the signal of the stator current, the electromagnetic torque, etc. The level numbers (N_{LN}) of decomposition, advisable is:

$$N_{LN} = \text{int}\left[\frac{\log\left(\frac{12.8\times10^3}{50}\right)}{\log(2)}\right] + 1 \; or \; 2 = 9 \; or \; 10 \; levels$$

According to Shannon's theorem, the details of frequencies are included in the following bands:

$$f_{di} \in \left[\left(\frac{f_{sa}}{2^{(i+1)}}\right) \rightarrow \left(\frac{f_{sa}}{2^i}\right)\right] Hz \quad (9)$$

The bands frequencies of the approximations signals a_j are the following:

$$f_{aj} \in \left[0 \rightarrow \left(\frac{f_{sa}}{2^{(j+1)}}\right)\right] Hz \quad (10)$$

Table (II) indicates to the different frequency bands:

Table II. Different frequency bands of levels

Frequency bands of level decomposition (Hz)	
d_7	50 - 100
d_8	25 - 50
d_9	12.5 - 25

We used the mother wavelet Daubechies 44 (db 44) for the decomposition into multi-level of the stator current.

Figures (9) and (10) show the DWT decomposition of the stator current for a healthy and faulty state under 0% of the load and at 75% of the load operation. The figures show the details of d1 to d9 with the approximation a9.

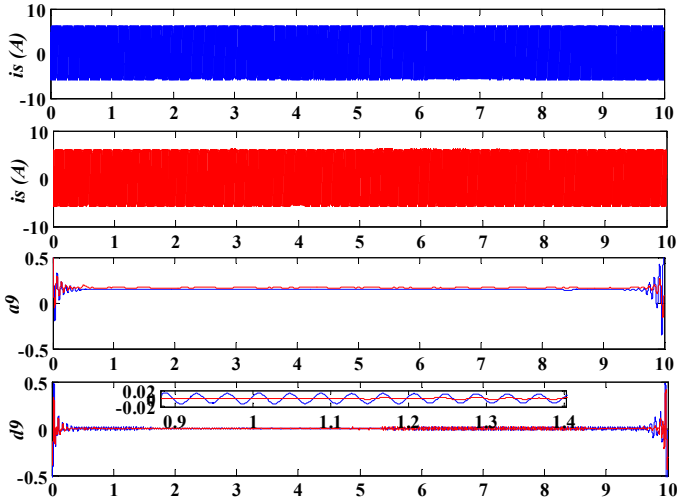

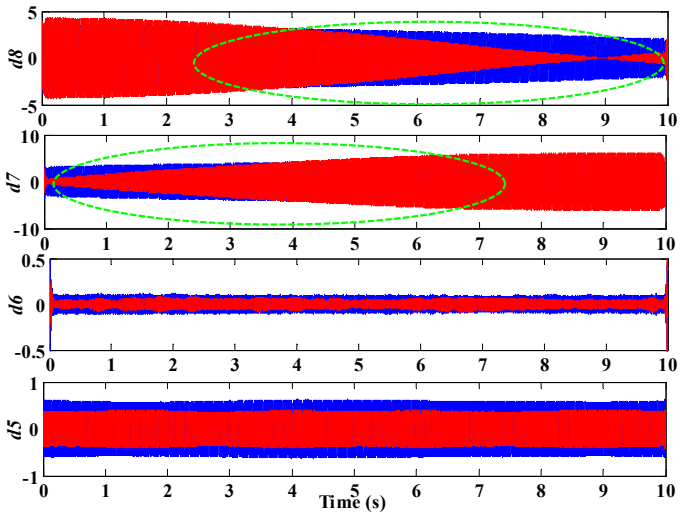

Figure 9. DWT analysis of stator current at 0% of the load (healthy: blue; 1BRB: red)

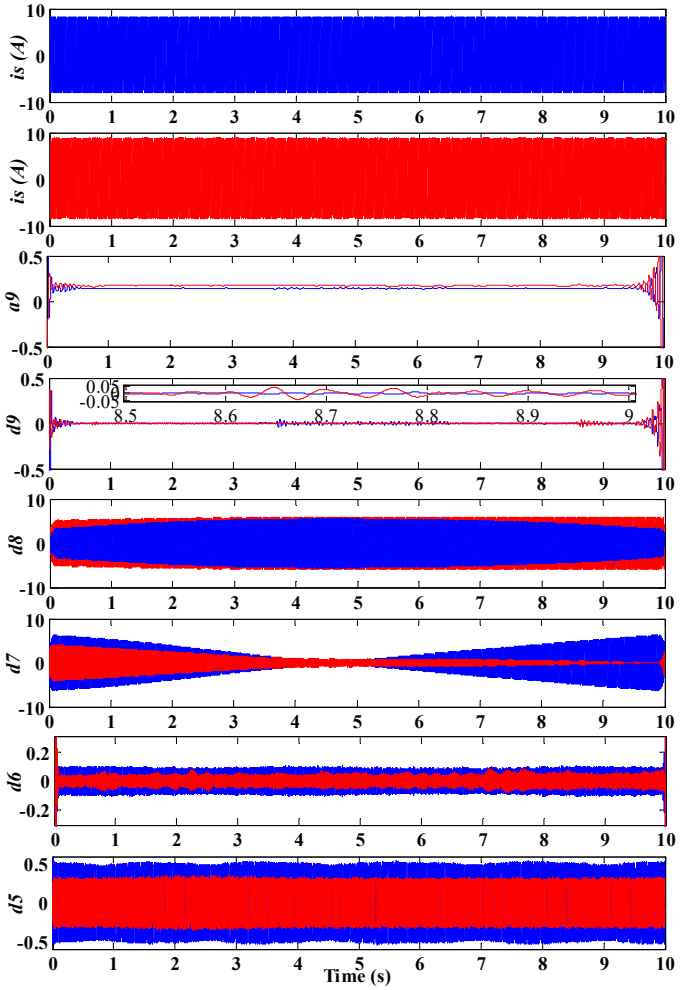

Figure 10. DWT analysis of stator current at 75% of the load (healthy: blue; 1BRB: red)

The different conditions of the induction motor (1BRB, 0% or 75% of the load) show well the evolution of the signals. Based on Figures (9) and (10) which show the details of d5 to d9 and the approximation a9; we see that the analysis results give a clear variation at the level of d5, d6, d7, d8, d9 and a9, with a slight change for the others (by vision). The frequency bands affected are:

d_5	200 - 400
d_6	100 - 200
d_7	50 - 100
d_8	25 - 50
d_9	12.5 - 25

A. *Details Energy*

We can calculate the energy of every detail to find a new indicator. The Calculation of each energy value is based on:

$$E_j = \sum_{n=1}^{N} \left| d_j(n) \right|^2 \qquad (11)$$

Where j is the level of detail, d_j is the detail signal at level j and N is the total number of samples in the signal.

Fig. 11 and Fig. 12 illustrate the variation of the energy for two conditions of the induction motors (healthy and faulty state). We can notice the difference between the energies in healthy and faulty cases. The information of BRB fault is revealed and the energy variation of *d7* is remarkable. There are a changed in the energies of d5 and d8 also. So, fault detection is possible by the analysis of d5 and d8.

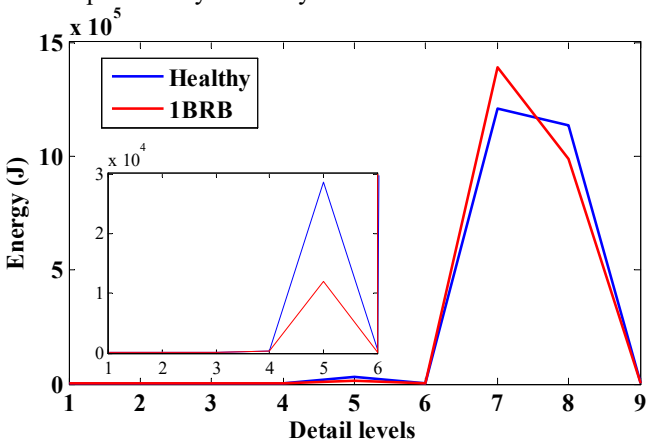

Figure 11. Energy level from 1 to 9 of stator current at 0% of the load

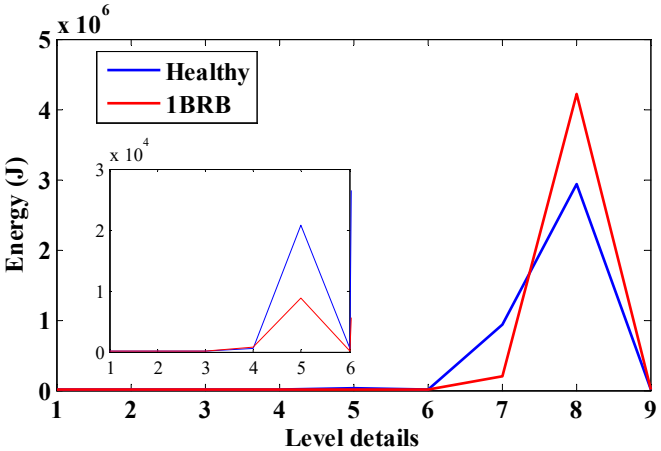

Figure 12. Energy level from 1 to 9 of stator current at 75% of the load

We calculated the energy of each detail. The objective is to compare the both amplitudes of the energy in a healthy and faulty state. This comparison allows us to verify how the frequency responsible bandwidth energy level. We can stop at *d6* to show the difference and to find the fault information.

B. Mean Square Error 'MSE'

Several methods are used in order to compare between many signals. Among them, we find the analysis by the mean squared error estimator 'MSE'. This factor can be used as a quality and/or quality indicator by a percentage of correspondence between the signals.

Mean square error (MSE) is a frequently measure used in order to verify the difference between the values predicted by a model in the healthy state and the values of faulty state [29]. The resemblance coefficient of MSE for two signals X_1 and X_2 (in each position i) which have a point numbers n is calculated by the following formula:

$$MSE = \frac{\sum_{i=1}^{n} (X_{1,i} - X_{2,i})^2}{n} \quad (12)$$

We have used this indicator for any detail di to determine the frequency band on the one hand and on the other hand for the determination of the dominant detail in the new signal.

We can report to other indicators such as: Root Mean Square Error (RMSE) and Normalized Mean Square Error (NMSE).

Our analysis of the BRB defect will be based on the MSE value for detail signals. The resemblance of the signals is checked for MSE value that tends to zero.

Details and approximations provide much information on the existence of the BRB faults.

These figures below summarize the qualitative and quantitative aspects of our analysis by the MSE values.

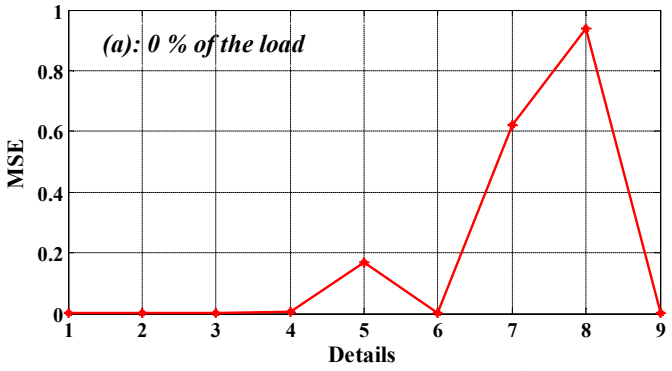

Figure 13. MSE evolution for 1BRB at 0% of the load

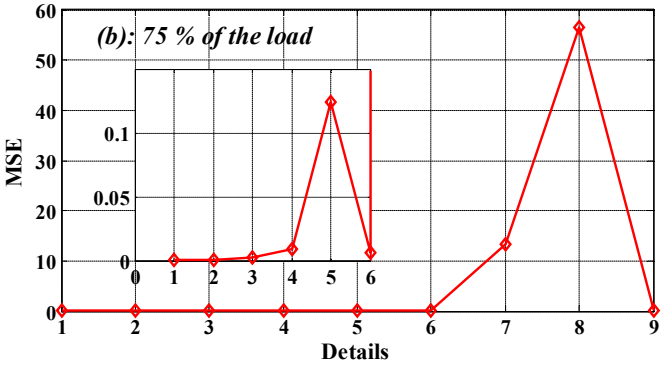

Figure 14. MSE evolution for 1BRB at 75% of the load

The discrete wavelet transform analysis is a very effective tool for the detection of the BRB faults. Especially, the introduction of the mean square error gave a well indicator of BRB faults exists.

It has been noticed that the most significantly affected bands for this BRB fault analysis are 25 Hz to 100 Hz (d7 and d8). This frequency band explains the effect of the sideband frequencies around the fundamental frequency which have been found by the FFT method.

V. DETECTION OF BRB FAULTS USING EMD

Among the techniques used in the signal processing field the Hilbert-Huang transform (HHT) which has the objective of breaking down a signal into so-called intrinsic functions (IMFs) and to obtain instantaneous frequencies. It is able to work with non-stationary and / or nonlinear data, unlike other transforms such as the Fourier transform (FT). HHT has the advantage of being an algorithm or an empirical approach that can be applied to several data: theoretical or practical data.

HHT is based on empirical mode decomposition (EMD) which decomposes signals into various components. We can compare the EMD by other analysis methods such as the Fourier transform (FT) and the wavelet transform (WT). According to the EMD, any signal can decompose it down into a finite and often small number of components. In addition, they can be described as intrinsic mode functions (IMFs).

Since the first IMF usually carries the most oscillating components (high frequency), it can be rejected to remove high frequency components (eg. random noise). EMD is adaptive and very efficient in time and frequency domain. It can also be applied to non-linear and non-stationary processes.

The requirements that define an IMF are:

- Throughout the dataset, the number of extrema and the number of zero-crossings (ZC) must be equal to or differ at most by one.

- The mean value of the envelope defined by the local maxima and the envelope defined by the local minima is null in every point.

Generally, it represents a simple oscillatory mode. By definition, an IMF is a function with the same number of extrema and zero-crossings, whose envelopes are symmetrical with respect to zero. This definition guarantees a good Hilbert transformation of the IMF.

The extraction steps of an IMF are called sieving. The screening process is to follow the following points:

1- Identify all local extrema in the test data.

2- Connect all local maxima with a cubic spline line as the upper envelope.

3- Repeat the procedure for local minima to produce the lower envelope.

Some works exploit the extracted features from two of the obtained IMFs form the basis of the proposed classification criterion; such as the samples between zero crossings (SBZCs) and the time between successive zero crossings (TSZCs) [24].

The upper and lower envelopes must cover all the data between them. Their average is m1. The difference between the data and m1 is the first component h; m_1 is subtracted from the original signal as follows:

$$X(t) - m_1 = h_1 \tag{13}$$

If h_1 is not an IMF, the procedure must be repeated dealing with h_1 as if it was the original signal.

In this way, the mean of the envelopes of h_1 will be m_{11} and h_{11} is computed:

$$h_1 - m_{11} = h_{11} \tag{14}$$

We verify that h_{11} is satisfied with the conditions that must be considered an IMF. The procedure will be repeated k times if h_{11} is not an IMF:

$$h_{1(k-1)} - m_{1k} = h_{1k} \tag{15}$$

when h_{1k} satisfies the IMF conditions, then:

$$c_1 = h_{1k} \tag{16}$$

c_1 becomes the first IMF (IMF_1). It can be transformed into a signal modulated in pure frequency of constant amplitude. The iteration stop criterion is mandatory in order to guarantee the physical meaning of c_1.

This is accomplished by restricting the size of the SD computed between two consecutive iterations:

$$SD = \sum_{t=0}^{T} \left[\frac{\left(h_{1(k-1)}(t) - h_{1k}(t)\right)^2}{h_{1(k-1)}^2(t)} \right] \tag{17}$$

where,

SD = ~0.2 or 0.3.

To get the MFI, we make the subtraction between the original signal and c_1 which leads us to find the residue r_1.

$$X(t) - c_1 = r_1 \tag{18}$$

Generally, the residue r_1 contains important information. The IMF decomposition can be performed n times until the residue r_n becomes a monotonic function from which no new IMF can be extracted. The residue plus the extracted n IMF can reconstruct the original signal by the following formula:

$$X(t) = \sum_{i=}^{n} c_i + r_n \tag{19}$$

After n number of IMFs extracted which are simple oscillatory functions with instantaneous amplitude (IA) and instantaneous frequency (IF); we found r_n which is the residue of data x(t).

As the EMD does it an adaptive process and so that each IMF generated from the information of the same signal processed. Unlike the wavelet transform which must define a mother function.

The EMD of the stator current (original signal) is shown in figure (15) with 7 IMFS. In this figure, the stator current processed for 10 seconds of the healthy state and with 0% of the load motor. In addition, figure (16) shows the condition where the induction motor is under 1BRB.

The IMFs shapes between two cases shows the difference between them for the healthy state and the defective state of the induction motor

Exploitation of these signals (IMFs) is the subject of several researchers

It is important to notice that BRB faults is clear in IMF2, IMF3, IMF4, IMF5, IMF6, IMF7.

This information on the existence of the BRB fault is difficult to find by the MCSA-FFT technique.

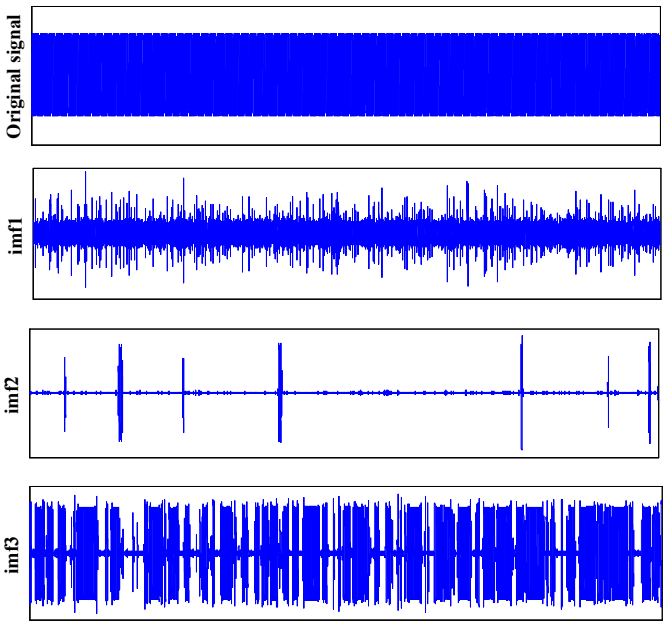

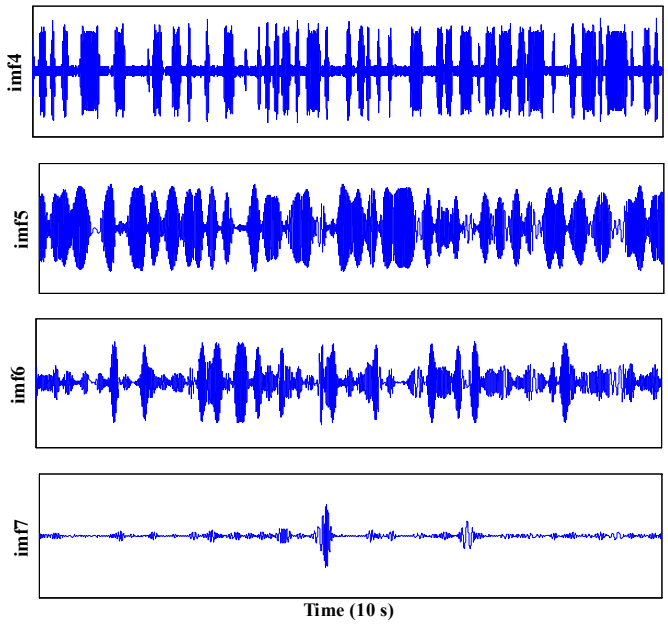

Figure 15. EMD of stator current with healthy motor and at 0% of load

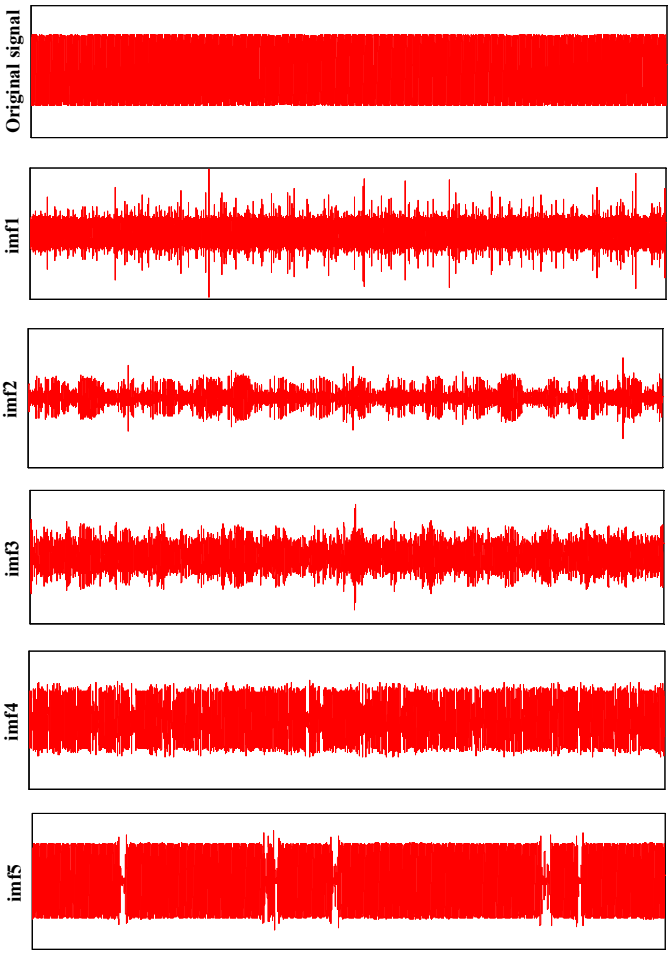

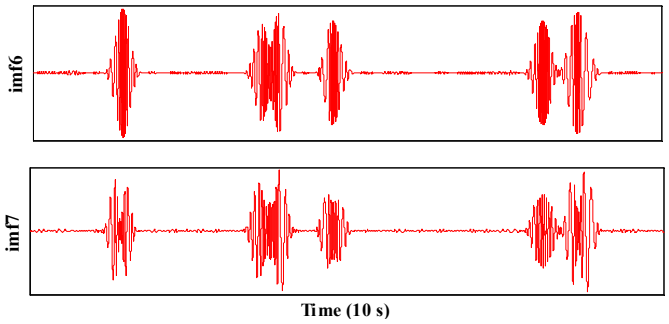

Figure 16. EMD of stator current with 1BRB and at 0% of load

We can now load this motor with a suitable brake, that is to say it applies a resistant torque. When increasing the resistive torque (to 75% of the load).

In this case, the slip will be different from zero. The shape of the instantaneous current in the healthy state is represented in figure (16).

In the same way, we present the stator current in the defective case (1BRB) of the induction motor.

IMFs from 2 to 7 appear clearly different between the healthy and faulty machine. This information is very interesting; they are considered as an indicator that ensures the detection of the BRB faults.

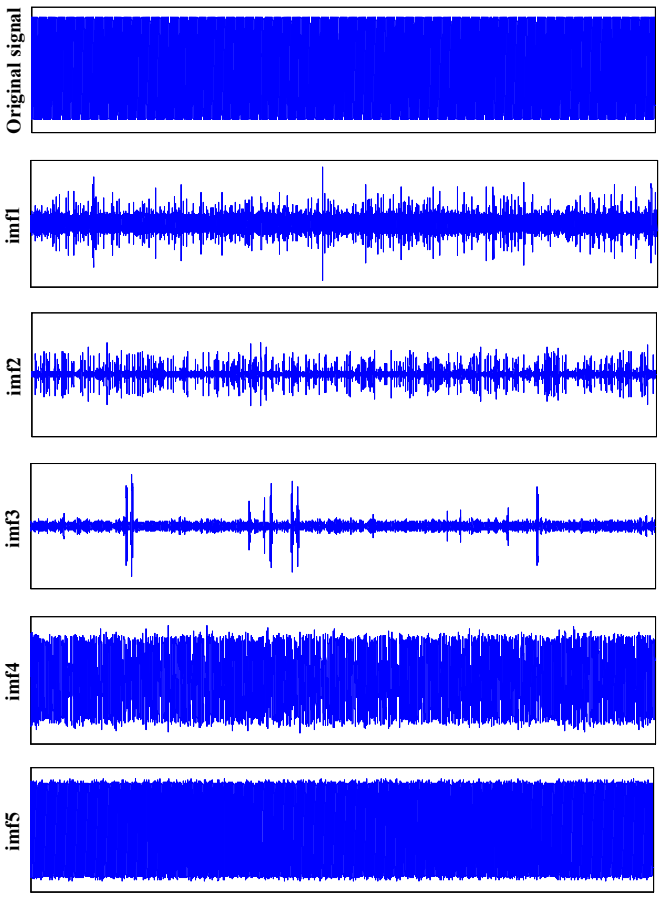

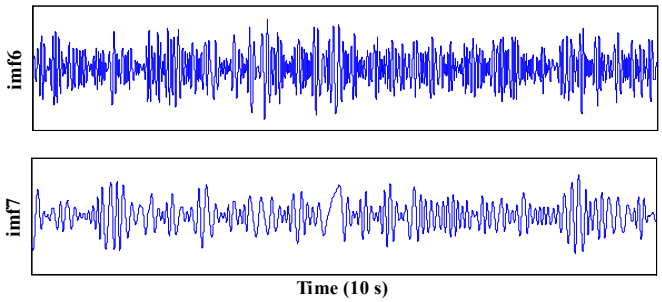

Figure 17. EMD of stator current with healthy motor and at 75% of load

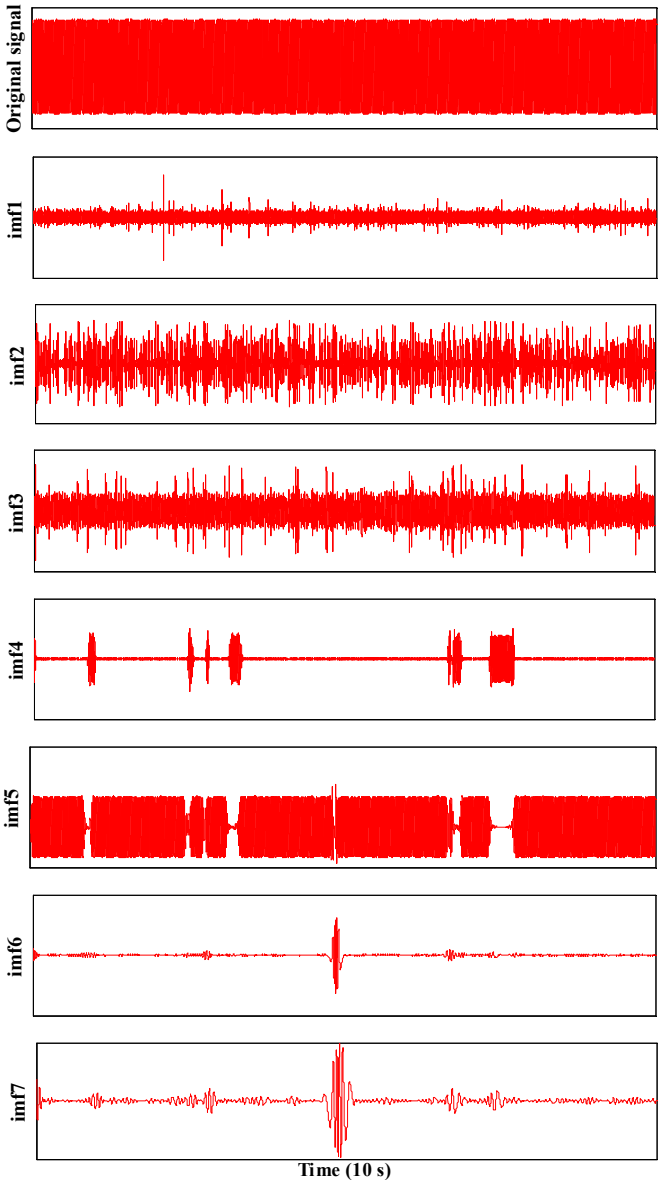

Figure 18. EMD of stator current with 1BRB and at 75% of load

The analysis results of experimental data indicate that the EMD method has a better performance and also can be successfully applied to stator current analysis.

VI. Conclusion

The FFT was applied to the stator current signal to determine the frequency content.

According to the creation of BRB faults in SCIM; MCSA-FFT technique shows good correspondence and accuracy with the literature studies. Frequency formulas, the harmonic displacement and the degree of severity of the broken rotor bar faults are checked.

It is important to notice that the presence or absence of the characteristic frequencies is dependent on the operating mode (at no-load or load motor). So, it is very difficult to detect this defect by MCSA at no-load operation of the induction motor. In addition, this technique is not valid in the non-stationary regime.

DWT has been applied to analyze the stator current more efficiently in detail. According to the figures which indicate the MSE values, we saw the influence of the load on d7 and d8. A new indicator has been applied which based on a well-defined value. MSE value is a quantitative indication which is reflected by qualitative terms.

The analysis of the stator current in induction motor using the DWT technique is adequate to detect the BRB faults. DWT is sensitive to any change in the stator current signal. In addition, DWT is effective for both operation regimes: stationary and non-stationary.

The analysis results of experimental data indicate that the EMD technique has a better performance and can be successfully applied to stator current analysis.

As DWT, the EMD technique is very efficient for non-stationary signals. The advantages of DWT and EMD techniques are considered an important benefit compared to the MCSA method.

Acknowledgment

We thank our colleagues from laboratory LGEB (University of Biskra) who provided insight and expertise that greatly assisted the research, although they may not agree with all of the interpretations/conclusions of this paper.

References

[1] A. M. Júnior, V.V. Silva, L.M. Baccarini, L.F.Mendes, “The Design of Multiple Linear Regression Models using a Genetic Algorithm to diagnose Initial Short-Circuit Faults in 3-Phase Induction Motors,” *Applied Soft Computing*, pp. 50-58, 2018.

[2] H. H. Eldeeb, H. Zhao, O. Mohammed, “Effect of Stator's Insulation Failure on the Performance of Motor Drive system,” *IEEE International Applied Computational Electromagnetics Society Symposium (ACES)*, pp. 1-2, 2020.

[3] G. Singh, V. N. A. Naikan., “Detection of Half Broken Rotor Bar Fault in VFD Driven Induction Motor Drive using Motor Square Current MUSIC Analysis,” *Mechanical Systems and Signal Processing*, pp. 333-348, 2018.

[4] N. Bessous, S.E. Zouzou, S. Sbaa, W.Bentrah, Z. Becer, R. Ajgou, “Static Eccentricity Fault Detection of Induction Motors using MVSA, MCSA and Discrete Wavelet Transform (DWT),” *in Electrical Engineering Conference -Boumerdes (ICEE-B)*, *IEEE*, 2017, pp. 1-10.

[5] F. Filippetti, F., M. Martelli, G. Franceschini, C. Tassoni., “Development of Expert System Knowledge Base to On-Line Diagnosis of Rotor Electrical Faults of Induction Motors,” *in Industry Applications Society Annual Meeting Conference*, *IEEE*, 1992 pp. 92-99.

[6] N. Bessous, S.E. Zouzou, S. Sbaa, A. Khelil, "New Vision about the Overlap Frequencies in the MCSA-FFT Technique to Diagnose the Eccentricity Fault in The Induction Motors," *in Electrical Engineering Conference*, *IEEE*, 2017, pp. 1-6.

[7] M. Deeb, N.F. Kotelenets, "Fault Diagnosis of 3-phase Induction Machine Using Harmonic Content of Stator Current Spectrum," *IEEE International Youth Conference on Radio Electronics, Electrical and Power Engineering (REEPE)*, pp. 1-6, 2020.

[8] N. Bessous, S. E. Zouzou, S. Sbaa, W. Bentrah., "A Comparative Study between the MCSA, DWT and the Vibration Analysis Methods to Diagnose the Dynamic Eccentricity Fault in Induction Motors," *in Systems and Control Conference (ICSC)*, *IEEE*, 2017, pp. 414-421.

[9] Y. Hu, C. Fangsen, X. Tu, F. Li, "Bayesian estimation of instantaneous speed for rotating machinery fault diagnosis," IEEE Transactions on Industrial Electronics, 2020.

[10] J. Martinez, A. Belahcen, A. Muetze, "Analysis of the Vibration Magnitude of an Induction Motor with Different Numbers of Broken Bars," *IEEE transactions on industry applications*, pp. 2711-2720, 2017.

[11] M. Akar, H.S. Gercekcioglu, "Instantaneous Power Factor Signature Analysis for Efficient Fault Diagnosis in Inverter Fed Three Phased Induction Motors," *International Journal of Hydrogen Energy*, pp. 8338-8345, 2017.

[12] M. Dybkowski, K. Klimkowski, "Speed Sensor Fault Detection Algorithm for Vector Control Methods Based on the Parity Relations," *in Power Electronics and Applications Conference*, *IEEE*, 2017, pp. P-1.

[13] M. Mohamed, E. Mohamed, A.A. Mohamed, M. Abdel-Nasser, M.M. Hassan, "Detection of Inter Turn Short Circuit Faults in Induction Motor using Artificial Neural Network," *The 26th Conference of Open Innovations Association (FRUCT), IEEE*, pp. 297-304, 2020.

[14] S. S. Shetgaonkar, "Fault Diagnosis in Induction Motor using Fuzzy Logic," *in Computing Methodologies and Communication Conference (ICCMC)*, *IEEE*, 2017, pp. 289-293.

[15] G. H. Bazan, P.R. Scalassara, W. Endo, A. Goedtel, W.F. Godoy, R.H.C. Palácios, "Stator Fault Analysis of Three-Phase Induction Motors using Information Measures and Artificial Neural Networks," *Electric Power Systems Research*, pp. 347-356, 2017.

[16] H.D. Rações, F.J. Ferreira, J.M. Pires, C.V. Damásio, "Application of Different Machine Learning Strategies for Current-and Vibration-based Motor Bearing Fault Detection in Induction Motors," *In IECON 2019-45th Annual Conference of the IEEE Industrial Electronics Society*, pp. 68-73, 2019.

[17] N. Bessous, A. Chemsa, S. Sbaa, S., "December. New Vision about the Mixed Eccentricity Fault Causes in Induction Motors and its relationship with the Rolling Element Bearing Faults: Analytical model dedicated to the REB faults," *IEEE International Conference on Communications and Elec trical Engineering (ICCEE)*, pp. 1-11, 2018.

[18] Y. Park, M. Jeong, S.B. Lee, J.A. Antonino-Daviu, M.Teska, "Influence of Blade Pass Frequency Vibrations on MCSA-Based Rotor Fault Detection of Induction Motors," *IEEE Transactions on Industry Applications*, pp. 2049-2058, 2017.

[19] N. G. Lo, A. Soualhi, , M.Frinì, H., Razik, "Gear and Bearings Fault Detection using Motor Current Signature Analysis," *in Industrial Electronics and Applications Conference*, *IEEE*, 2018.

[20] A. Mejia-Barron, M. Valtierra-Rodriguez, D. Granados-Lieberman, J.C. Olivares-Galvan, R. Escarela-Perez, "The Application of EMD-Based Methods for Diagnosis of Winding Faults in a Transformer using Transient and Steady State Currents," *Measurement*, pp. 371-379, 2018.

[21] P. S. Panigrahy, P. Konar, P. Chattopadhyay, "Broken Bar Fault Detection using Fused DWT-FFT in FPGA Platform," *in Power, Control and Embedded Systems Conference (ICPCES)*, *IEEE*, pp. 1-6, 2014.

[22] A.E. Treml, R.A. Flauzino, G.C. Brito, "EMD and MCSA Improved via Hilbert Transform Analysis on Asynchronous Machines for Broken Bar Detection Using Vibration Analysis," *IEEE Milan PowerTech*, pp. 1-6, 2019.

[23] J. Faiz, V. Ghorbanian, B.M. Ebrahimi, "EMD-Based Analysis of Industrial Induction Motors with Broken Rotor Bars for Identification of Operating Point at Different Supply Modes," *IEEE Transactions on Industrial Informatics*, pp. 957-966, 2014.

[24] R. Valles-Novo, J. de Jesus Rangel-Magdaleno, J.M. Ramirez-Cortes, H. Peregrina-Barreto, R. Morales-Caporal, "Empirical Mode Decomposition Analysis for Broken-Bar Detection on Squirrel Cage Induction Motors," *IEEE Transactions on Instrumentation and Measurement*, pp. 1118-1128, 2015.

[25] W. Deleroi, "Broken Bar in Squirrel Cage Rotor of an Induction Motor, Pan I: Description by Superimposed Fault Currents," *Arch. fur Elektrotechnik*, pp. 91-99, 1984.

[26] L. Abdesselam, G. Clerc, "Study of Rotor Asymmetry Effects of an Induction Machine by Finite Element Method," *Journal of Electrical Engineering and Technology*, pp. 342-349, 2011.

[27] J. A., Antonino-Daviu, M. Riera-Guasp, J. R. Folch, M. P. M. Palomares, "Validation of a New Method for the Diagnosis of Rotor Bar Failures Via Wavelet Transform in Industrial Induction Machines," *IEEE Transactions on Industry Applications*, pp. 990-996, 2006.

[28] N. Bessous, S. E. Zouzou, W. Bentrah, S. Sbaa, M. Sahraoui, "Diagnosis of Bearing Defects in Induction Motors using Discrete Wavelet Transform," *International Journal of System Assurance Engineering and Management*, pp. 335-343, 2018.

[29] N. Bessous, S. Sbaa, S.E. Zouzou, W. Bentrah, Z. Becer, L. Zarour, "Application of New Quantitative and Qualitative Study Based on DWT Method To Diagnose the Eccentricity Fault in Induction Motors," *in Electrical Engineering Conference (ICEE-B)*, *IEEE*, 2017, pp. 1-6.